Pure appl. geophys. 158 (2001) 1763–1782
0033–4553/01/101763–20 $ 1.50 + 0.20/0

Pure and Applied Geophysics

Modelling of Seismic Ground Motion in Santiago de Cuba City from Earthquakes in Oriente Fault Seismic Zone

LEONARDO ALVAREZ,[1,4] GIULIANO F. PANZA,[2,3] FRANCO VACCARI,[2,4] and BERTHA E. GONZÁLEZ[1]

Abstract — We present the results of complete *P-SV* and *SH* waves modelling, up to a maximum frequency of 1 Hz, along two profiles in Santiago de Cuba city. The seismic sources are located in the depth range from 10 to 40 km on the Oriente fault zone at distances of several tens of kilometres from the city. The calculation has been made by a hybrid method: Modal summation in the regional anelastic model (one-dimensional) where the source is buried, and finite differences in the local sedimentary anelastic models (two-dimensional). The analysis of the influence of the depth and of the distance of the source on the site effects shows that standard traditional methods, based on the deconvolution analysis of the rock outcrop motion, can lead to erroneous results.

Key words: Synthetic seismograms, surface waves, microzoning, Santiago de Cuba.

1. Introduction

Santiago de Cuba is Cuba's second largest city. Located on an active earthquake zone, it has experienced the damaging effects of earthquakes since its foundation in the XVI Century and partial destruction during the earthquakes of 1776 ($M_I \cong 7.6$), 1852 ($M_I \cong 7.2$) and 1932 ($M_s = 6.75$). Furthermore, there exists a high probability of occurrence of an $M_s = 7$ earthquake in the near future (RUBIO, 1985) on the Oriente Fault system located immediately to the South of the city. For this reason several microzoning studies, based mainly on the analysis of engineering-geological conditions, real earthquake effects and microseism registrations, have been performed. The first complete microzoning of Santiago de Cuba was made by GONZÁLEZ *et al.* (1989), in the form of maps of the expected distribution of seismic intensity and of the predominant frequency of shaking, based on microseism analysis. Recently, by reprocessing all previous results with the aid of a GIS, a map that characterises the expected behaviour of soils was compiled (ZAPATA, 1996).

[1] Centro Nacional de Investigaciones Sismológicas, Cuba.
[2] Department of Earth Sciences, University of Trieste, Italy.
[3] The Abdus Salam International Centre for Theoretical Physics, SAND Group, Trieste, Italy.
[4] Gruppo Nazionale per la Difesa dai Terremoti, Italy.

Until the present, synthetic seismograms were obtained in two ways: (a) by the scaling of weak earthquakes registered on rock (a seismic station located 18 km from the city) to unconsolidated sediments by considering the transfer functions determined from microseisms (GONZÁLEZ, 1991); (b) by applying a semi-empirical method developed by TRIFUNAC (1977) which considers only distance, magnitude and soil kind (ZAPATA, 1996). There are no available seismic records from the city that may be used as a calibration of the computed seismograms.

The methods just mentioned neglect source (focal mechanism and duration) as well as path (regional structure) effects that may have a large influence on the local ground motion. To take into account these effects, we use a method for the calculation of synthetic seismograms in laterally variable anelastic media known as the "hybrid technique" (FÄH, 1992; FÄH *et al.*, 1993; FÄH and SUHADOLC, 1994). The main idea is to calculate complete wavetrains generated by a seismic source buried in a regional crust-upper mantle structure, the bedrock structure, and to apply this motion as input to the local structure. The problem is solved in two steps: (a) the *P-SV* and *SH* waves signals are generated in the bedrock anelastic structure by the modal summation approach (PANZA, 1985; FLORSCH *et al.*, 1991); (b) these wavetrains are used as input for a finite-difference scheme that is used to obtain the waveforms along the local, laterally varying anelastic structure (FÄH, 1992; FÄH *et al.*, 1993).

2. Geological Setting

The territory of the city of Santiago de Cuba and its surroundings covers an area of about 250 km^2 and is characterised, from the geological point of view, by rocks, and stiff and unconsolidated sediments of different age, origin and lithological composition.

The oldest rocks that outcrop in the studied territory are classified as tertiary and belong to the "El Cobre" formation, composed mainly of volcano-clastic rocks (various kinds of tuffs, tuffites and agglomerates) of basic and intermediate composition, with intrusions of diorites and granodiorites. The thickness of this formation exceeds 1000 m. The "La Cruz" formation overlays, in a discordant way, El Cobre formation, and is mainly composed of calcareous conglomerates and sandstones in its lower part, and by organic limestones in its uppermost part. When the limestones outcrop they appear intensively meteorised (calcareous eluvium). The thickness of this formation is about 100 m.

The "Santiago" formation is represented by stiff Pliocene clays and sandy clays, with a thickness ranging from 10 to 50 m. The formation outcrops in the northeastern part of the territory, where a considerable part of the urbanised area is located.

The Quaternary sediment formations are of two types. The first one mainly comprises gravelly alluvium (gravels, sands and clays with calcareous composition).

These soils are found mostly filling river basins such as the San Juan River basin in the eastern part of the city and they are some 20–30 m thick. The other kind of Quaternary sediments can be identified bounding the Santiago de Cuba and Cabañas bays, and is composed of sandy clays and peat as well as man-made ground and bay mud. The thickness of this formation is about 5–10 m.

The Maya formation is composed in its lower part of dense calcareous conglomerates and gravelites and of hard and dense organic cavern limestones in its upper part. The thickness of this formation ranges from 30–50 m. Organic limestones with a wide development of surface karstic phenomena compose the "Jaimanitas" formation. Its thickness ranges between 2 and 20 m. These two formations are very well represented along the seacoasts of the studied territory. Figure 1 presents a simplified geological scheme of Santiago de Cuba basin.

3. Regional Structural Model

The bedrock regional structural model has been compiled from different sources. The uppermost 150 km are a slight modification of the *P*- and *S*-wave velocity model routinely used for the hypocenter's determination in eastern Cuba (MINBAS, 1989), the density values have been adapted from those proposed by ORIHUELA and CUEVAS (1993), and for all the layers $Q_\alpha = 400$ and $Q_\beta = 200$ (Fig. 2) have been assumed. The upper frequency limit for the numerical simulation has been fixed in 1 Hz, because the available structural model is not detailed enough to warrant computations reliable at higher frequencies. Our results can be directly applied to ten and more story buildings, lifelines, etc. This possibility is very important for Santiago de Cuba city, where approximately ten years ago a program of the construction of typical 12, 15 and 18-story buildings began, and measurements of microseisms show that free oscillation periods of 18-story buildings are in the range 0.8–1.2 seconds (GONZÁLEZ, 1998; SEO *et al.*, 1998). The completeness of the synthetic signals is granted by the depth extension of the considered earth model until 1200 km (PANZA, 1985).

4. Two-dimensional Structural Profiles in the City

In order to study the influence of local soil conditions on seismic input, we select two profiles in different parts of the city that cross the main structural formations (with the exclusion of the coastal Maya and Jaimanitas). Profile A, with a length of 12 km, extends along the San Juan River basin, while profile B, 10 km long, crosses the northern part of Santiago de Cuba bay through the industrial part of the city and some urbanised areas. The two profiles are located approximately 40 km and 80 km from sources A and B, respectively. The two sources belong to the Oriente transform fault system, where the expected strong earthquakes are likely to be located (Fig. 3).

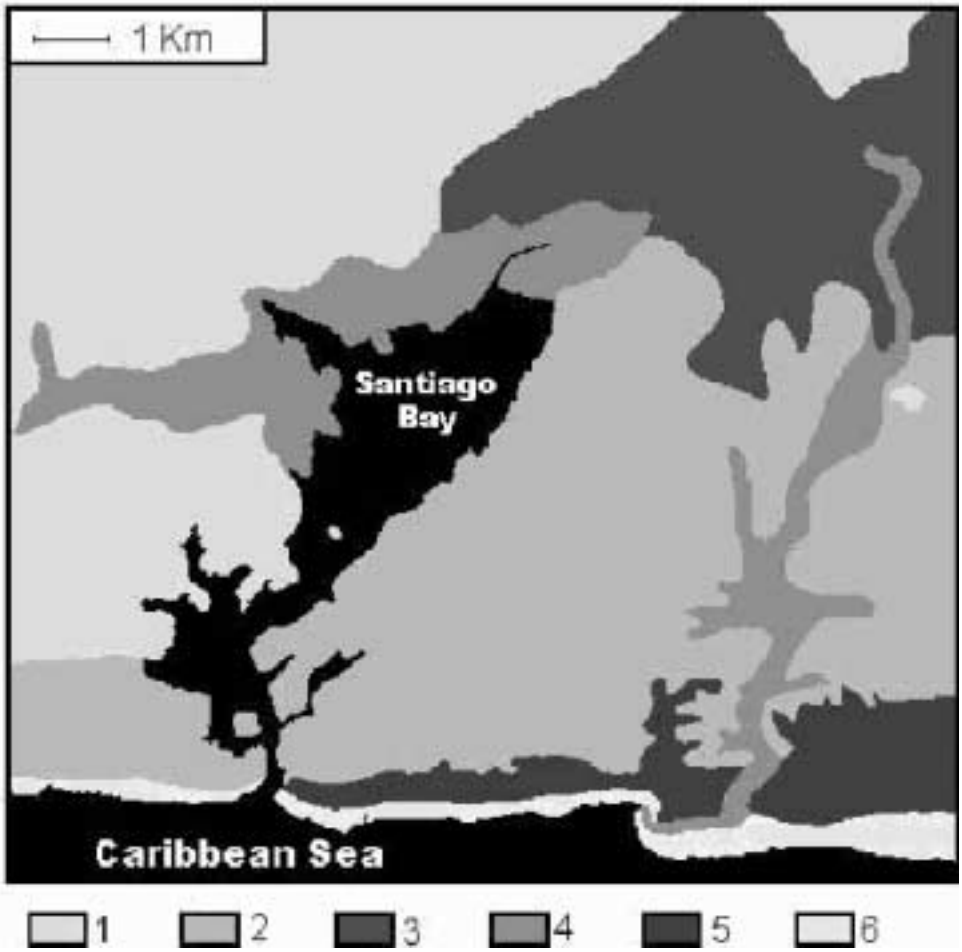

Figure 1
Geological scheme of the Santiago de Cuba basin [modified from HEREDIA *et al.* (1982)]. 1 – El Cobre formation, 2 – La Cruz formation, 3 – Santiago formation, 4 – Quaternary sediments formations, 5 – Maya formation, 6 – Jaimanitas formation. References in the text.

For both profiles a 200 m deep cross section has been constructed, considering the characteristic soils of Santiago de Cuba (GONZÁLEZ *et al.*, 1989) and with the aid of geotechnical boreholes data. The mechanical properties of the materials (*P*- and *S*-wave velocities and quality factors) have been selected from specialised literature (PAVLOV, 1984; ISHIHARA, 1993) and the density and porosity indexes are supported by laboratory measurements. The velocity values in rocks or soils are given in intervals, and to select a value in each case we take into account the density and the stiffness distribution over the boreholes used. This criterion also has been applied to

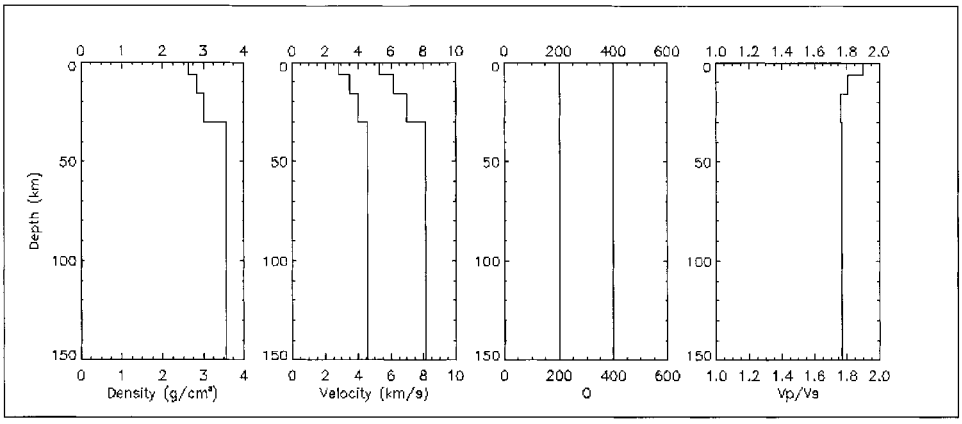

Figure 2
Regional bedrock structural model used in the calculations, details of the first 150 km.

quaternary sediments, and since they are mainly of calcareous composition, the obtained values may seem to be high.

5. P-SV and SH Waves Seismic Input Modelling

The hybrid approach developed by FÄH (1992) is used to model the seismic input in the investigated area. Wave propagation from the source up to the 2-D local structure is computed with the modal summation technique (PANZA, 1985; FLORSCH *et al.*, 1991), using the layered bedrock structure, representative of the path from the source to Santiago de Cuba, while finite differences are used to model the wavefield along the profiles selected in the city. The effectiveness of the boundary conditions applied to the model treated with the FD scheme is tested by computing, with the FD technique, the signals corresponding to the regional bedrock structure at selected sites along the profile, and comparing such results with the signals obtained with modal summation (for more details see FÄH, 1992).

The sites along both profiles are placed at intervals of 900 m. For each site we calculate displacement, velocity and acceleration seismograms for a point source with seismic moment $M_o = 1.0 \times 10^{13}$ N-m, focal depth $h = 30$ km, and focal mechanism: dip $= 21°$, azimuth $= 302°$ and rake $= 21°$. This mechanism corresponds to the Harvard University determination of one local earthquake that can be considered representative of sources A and B. These seismograms then have been scaled, in the frequency domain (PANZA *et al.*, 1996), for a possible earthquake of $M_s = 7.0$ ($M_o = 3.55 \times 10^{19}$ N-m) by applying the scaling law of GUSEV (1983), as reported by AKI (1987).

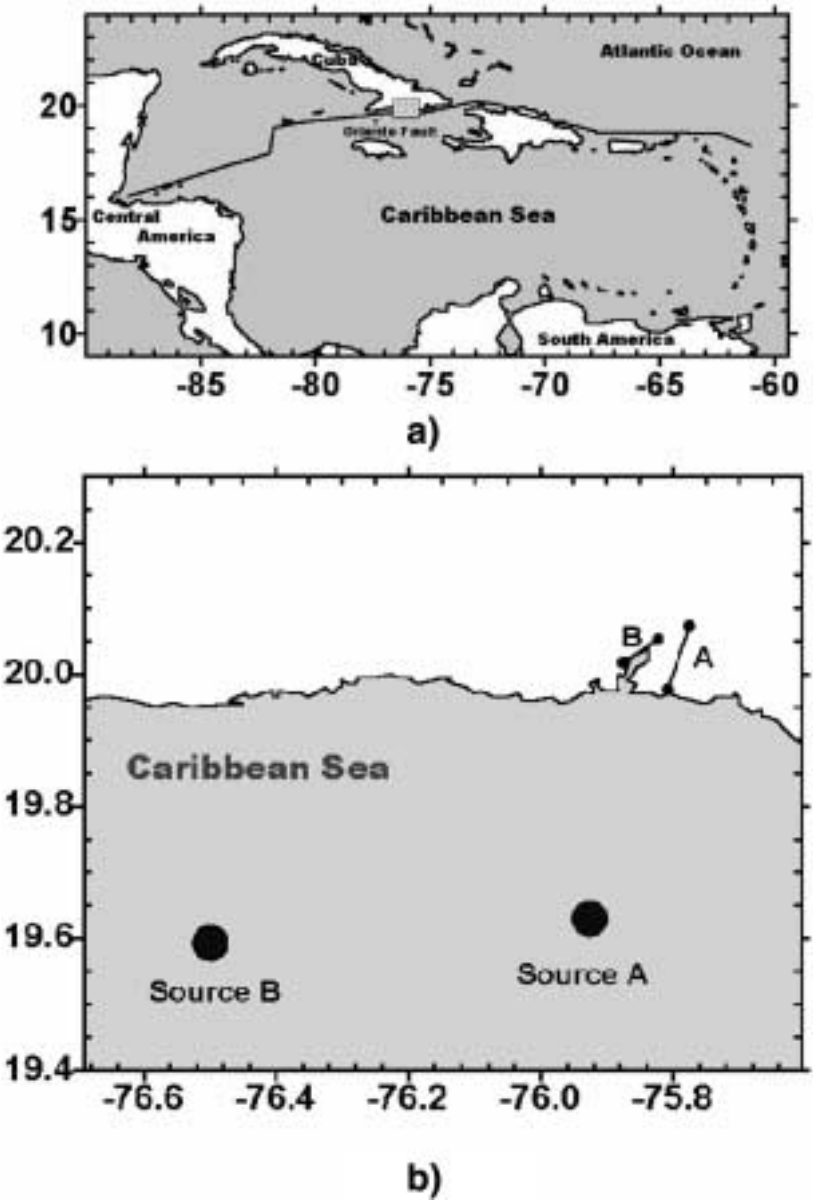

Figure 3
a) Geographical location of the study region; the solid line indicates a sector of the north boundary of the Caribbean plate, b) position of the profiles and of the sources considered.

6. Results

The lateral variations present in the local structures produce great variations in the seismograms. As could be expected, there is an increment of the signal duration and of the maximum amplitudes with respect to the bedrock signals, and in some cases the wave shape changes drastically (Fig. 4). Examples of velocity seismograms scaled for a $M_s = 7$ earthquake are shown in Figure 5. The maxima and minima of the peak values of ground motion and design ground acceleration (DGA) obtained by scaling acceleration seismograms with the design response spectra for rock sites of the Cuban building code (NORMA CUBANA, 1999), along both profiles, are given in Table 1. As a comparison, macroseismic intensities equivalent to displacement values have been determined from the relationships obtained by PANZA *et al.* (1997) and ALVAREZ *et al.* (1999) and are presented in Table 2.

In the frequency domain, in general, a sharp increase of the amplitudes ranging from 0.75–1.0 Hz is observed and at these frequencies the acceleration spectra are strongly dependent on the site, as can be seen from Figure 6.

Useful estimation of the local effects can be made by computing the response spectra ratio (RSR). For each site where we have made the computations we consider the spectral amplication defined by the ratio RSR = [RS(2D)]/[RS(1D)], where RS(2D) is the response spectrum (at 5% of damping) of the signal calculated for the laterally varying structure, and RS(1D) is the one calculated for the bedrock structure. In Figure 7 we show the RSR for the three components of motion along the two profiles.

7. Discussion

The RSR of Figure 7 show the influence of the soft sediments on ground motion. For frequencies below 0.4 Hz the RSR are very low, while large local maxima appear in the range 0.8–1.0 Hz. Along the profiles, the position of these maxima varies with varying components of motion. Along both profiles, the RSR maxima for vertical *P-SV* and *SH* waves are localised where there is a large variation of the relative thickness of the first two sedimentary layers, between sites 3 and 8. For the radial *P-SV* waves, the increment of the RSR in the sites with a strong gradient in the thickness of sediments appears as a local maximum, hidden by the absolute maximum at the end of the profile.

The peak amplitude values along each profile, given in Table 1, reveal that there is a wide variability, not only from site to site, but also between the different components. Along each profile, in spite of the multiplicity of conversion formulae considered to convert displacements into intensities, the seismic intensity varies only within one degree (Table 2).

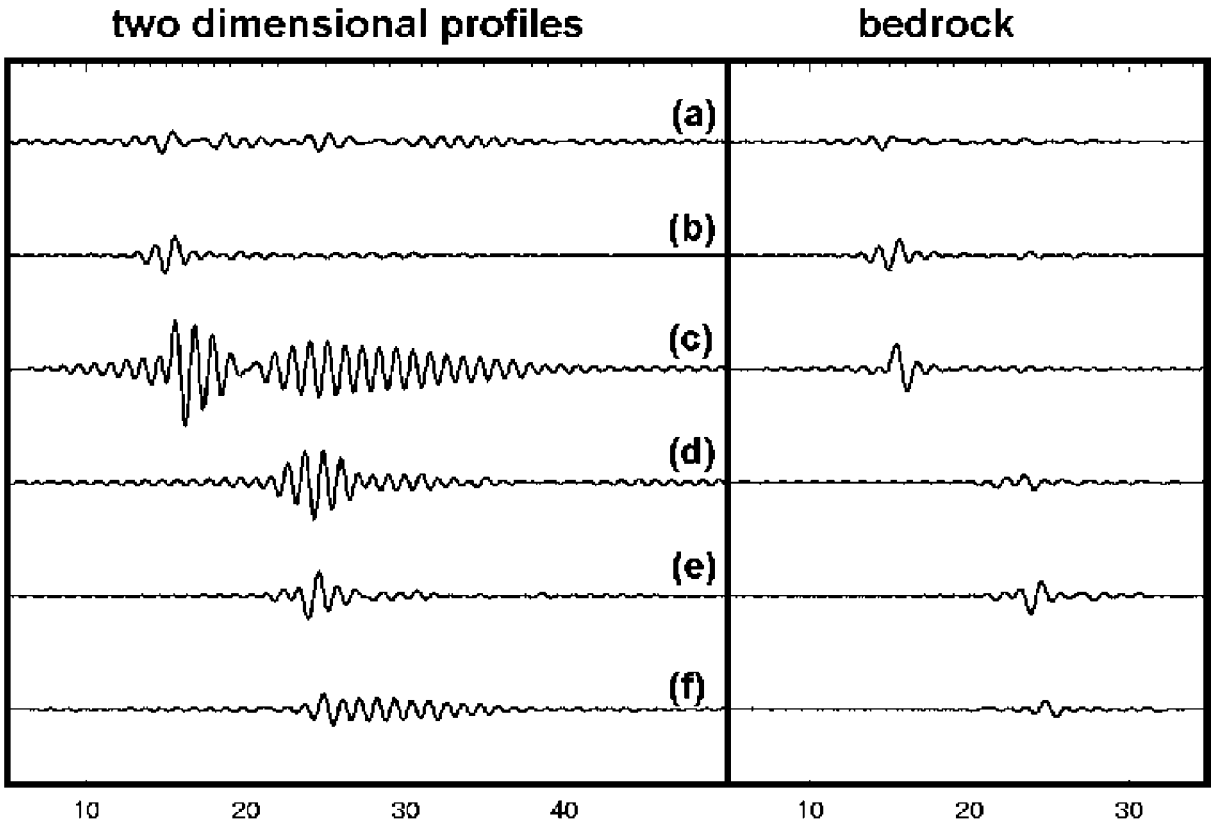

Figure 4
Comparison of velocity seismograms calculated for a $M_o = 1.0 \times 10^{13}$ N-m earthquake for points in the middle of both profiles with the ones calculated at equivalent distances in bedrock regional structure. Profile A: (a) radial, (b) vertical and (c) transverse. Profile B: (d) radial, (e) vertical and (f) transverse. All components are normalised to the absolute maximum (6.29×10^{-3} cm/sec.) of the set.

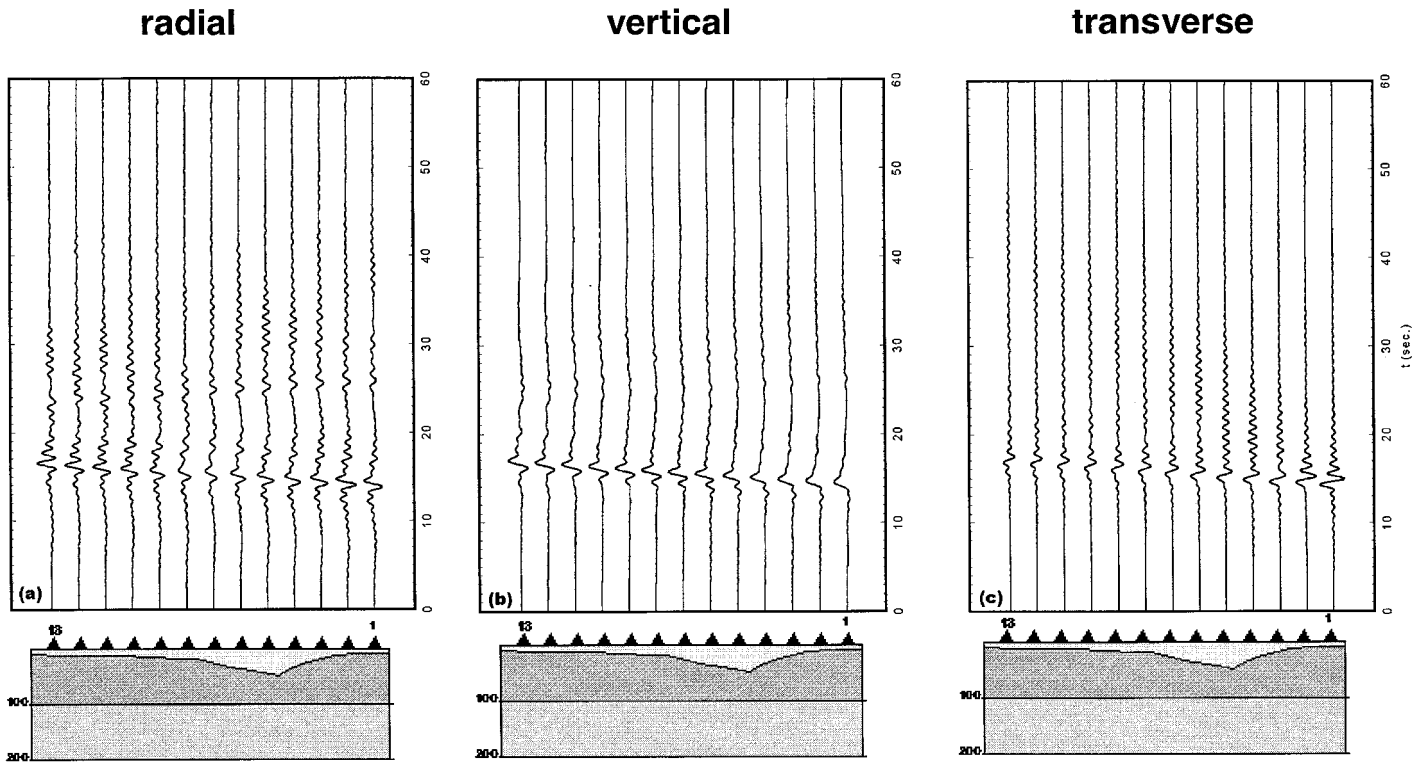

No	Density	Vp	Vs	Qp	Qs
1	1.8	1.7	0.4	100	50
2	2	1.9	0.6	200	100
3	2.3	2.2	0.8	400	200

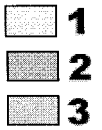

Figure 5
Expected ground-motion velocities normalised to maximum absolute peak amplitude (see Table 1) along the profile from an $M_s = 7$ earthquake. (a–c) profile A, San Juan River; (d–f) profile B, Santiago Bay. Cross sections and mechanical properties for each layer are also shown.

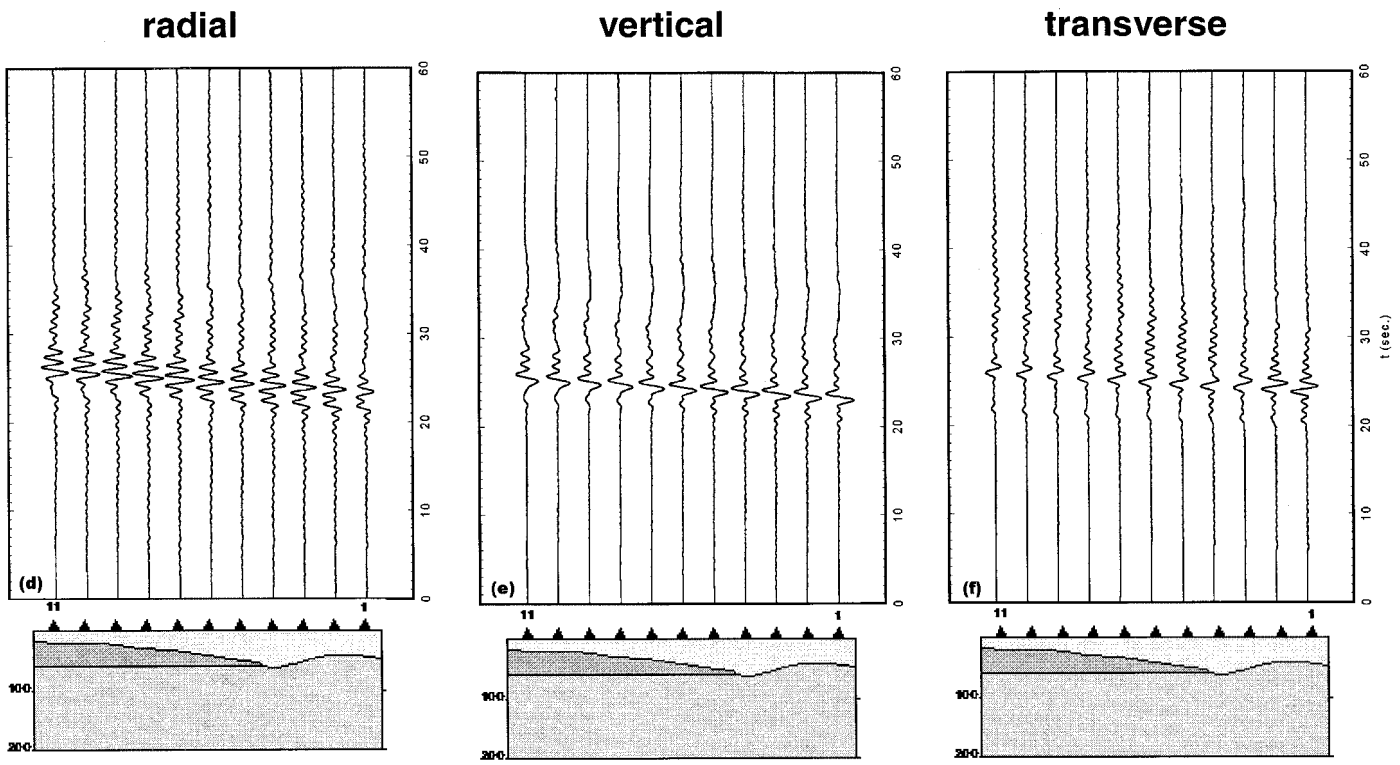

No	Density	Vp	Vs	Qp	Qs
1	1.85	1.8	0.5	100	50
2	2	1.9	0.6	200	100
3	2.3	2.2	0.8	400	200

Figure 5(d–f)

Table 1

Peak values for displacement D (cm), velocity V (cm/sec) acceleration A (cm/sec^2) for a maximum frequency of 1 Hz ([1]) and design ground acceleration DGA (cm/sec^2), along the considered profiles.

Comp. of motion	San Juan River (Profile A)				Santiago Bay (Profile B)			
	D	V	A	DGA	D	V	A	DGA
a) Maximum								
Radial	3.52	1.62	5.75	23.2	0.91	1.65	8.49	40.2
Vert.	5.95	1.53	4.69	15.6	1.32	1.63	6.63	20.4
Trans.	3.35	6.06	26.5	92.0	1.07	1.48	6.16	22.8
b) Minimum								
Radial	3.00	0.85	2.85	10.8	0.75	0.95	4.56	21.5
Vert.	1.13	1.27	2.64	7.0	0.78	1.21	4.70	15.0
Trans.	2.14	2.64	11.6	41.7	0.81	0.90	3.27	10.5

[1] It is well known that the acceleration at 1 Hz is not representative of the absolute maximum, that for this parameter of ground motion in general occurs at higher frequencies (e.g., PANZA *et al*., 1997). Nevertheless it can be extrapolated to high frequencies by using the design response spectra, commonly included in seismic building codes (a rough estimation of peak-ground acceleration can be obtained from maximum spectral value-*MSV*, through $MSV = 2.5 \times \text{DGA}$); a discussion of this procedure can be found in PANZA *et al*. (1996) and ALVAREZ *et al*. (1999).

7.1. Source Influence on Site Effects

Standard microzoning procedures more or less explicitly assume that the spectral ratios are independent from the source depth, distance and focal mechanism. This assumption may be acceptable when the subsurface geometry of the different lithologic units is simple and when single non-interfering seismic waves are

Table 2

Macroseismic intensities (MSK) converted from D values of Table 1 by using linear relationships of PANZA et al. (1997) (1, 2) and ALVAREZ et al. (1999) (3, 4). The values corresponding to each component and to the maximum of all components are given.

Comp. of motion	San Juan River (Profile A)				Santiago Bay (Profile B)			
	1	2	3	4	1	2	3	4
a) Maximum								
Radial	IX	VIII	VIII	VII	VI	VII	VI	V
Vert.	IX	VIII	IX	VIII	VII	VII	VII	VI
Trans.	VIII	IX	VIII	VII	VII	VI	VI	V
Max.	IX	IX	IX	VIII	VII	VII	VII	VI
b) Minimum								
Radial	VIII	VIII	VIII	VII	VI	V	VI	V
Vert.	VII	VI	VI	VI	VI	V	VI	V
Trans.	VIII	VII	VI	VI	VI	V	VI	V
Max.	VIII	VIII	VIII	VII	VI	V	VI	V

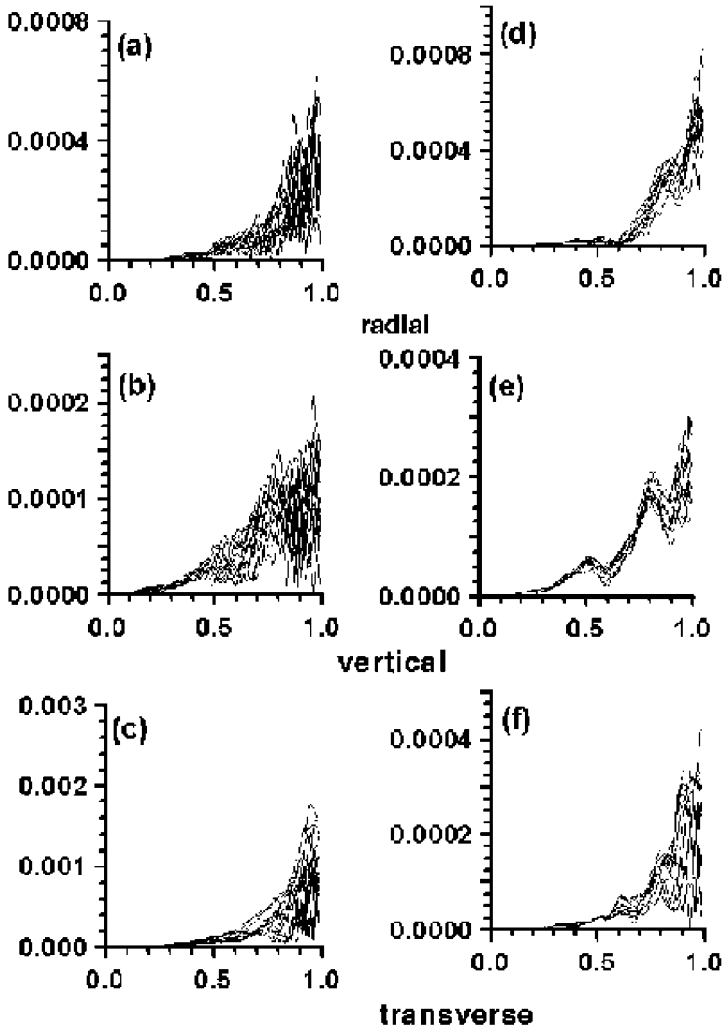

Figure 6
Acceleration amplitude spectra for the synthetic signals for a $M_o = 1.0 \times 10^{13}$ N-m earthquake in the considered sites along both profiles. (a), (b) and (c) profile A; (d), (e) and (f) profile B.

considered, however in general it represents an approximation too rough to allow reliable results to be obtained (PANZA *et al.*, 2000). This limit of standard microzoning procedures is evidenced by recent data that have shown that the recorded motions at the bedrock differ significantly from that obtained from a deconvolution analysis of the rock outcrop motion (FIELD, 1996; RIEPL *et al.*, 1998).

The effect of the source mechanism has been investigated in detail by ROMANELLI and VACCARI (1999) and PANZA *et al.* (1999). Here we consider the effect of the source position on RSR, performing the following tests.

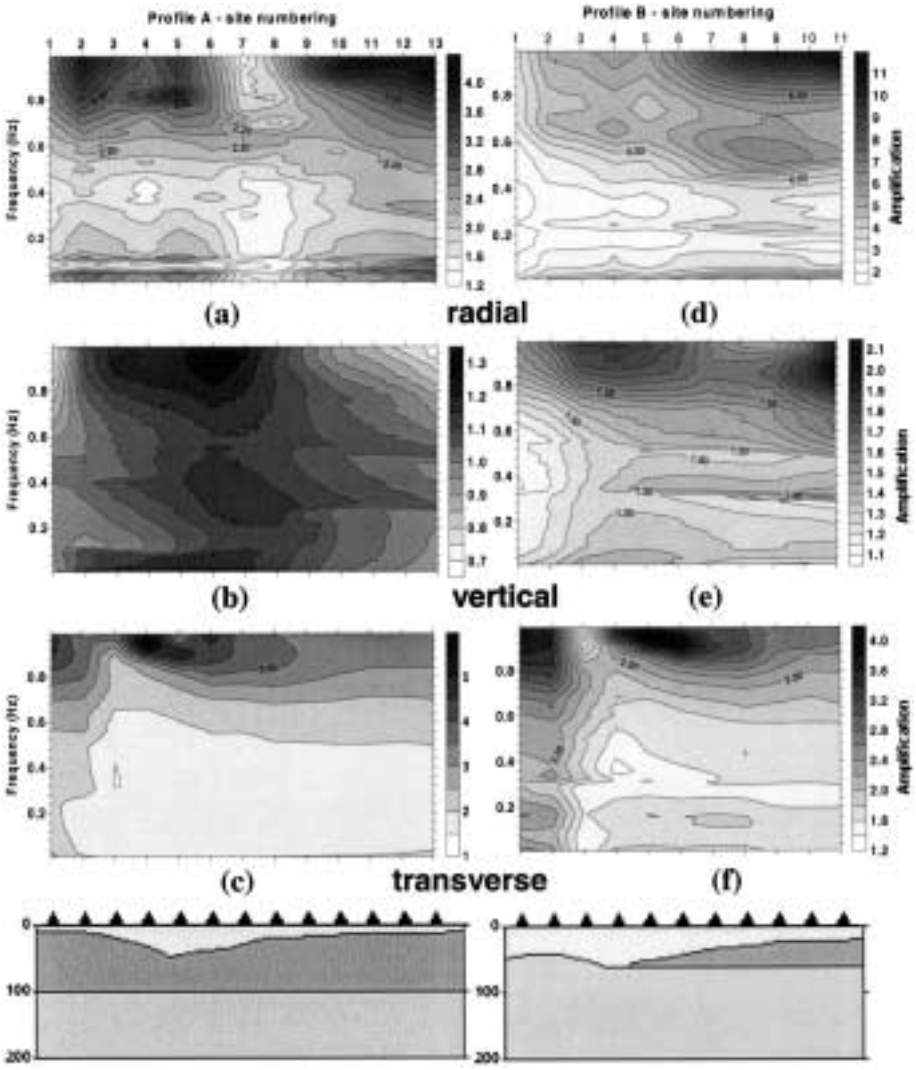

Figure 7
Relative response spectra as a function of frequency along each profile. (a), (b) and (c) profile A; (d), (e) and (f) profile B.

We analyse the influence of the source depth variation ranging from 10 to 40 km along profile B (on average about 85 km from the source). For depths ranging from 10 to 20 km and below 30 km, the large absolute maximum at about 10 km from the beginning of the profile (sites 10 and 11), clearly visible in Figure 7d, does not appear, and the absolute maximum is located between sites 2 and 5, in correspondence with the gradient of the thickness of the sediments. Therefore the large

maximum is clearly evident only if the source depth varies from 30 km to about 20 km (Figs. 7d, 8).

When the same analysis is performed for profile A, that on average is at about 45 km from the source, there are variations in the details of the picture of the RSR, nonetheless the main features remain visible, with the exception of the large maximum that now is absent.

Keeping the source at a depth of 30 km, we consider different distances, from the beginning of profile B, ranging from 40 to 120 km and we observe that the large absolute maximum is present for distances ranging from 60 to 120 km from the source. Similarly we can conclude that for profile A this critical distance varies in range from 70 to 90 km (Fig. 9).

Another test is made to investigate the profile geometry effects on polarization. We consider simple 1-layer and 2-layer structural models whose mechanical properties correspond to the different strata present in both profiles. Both El Cobre and La Cruz formations, alone or combined, give an RSR picture very close to the one presented in Figure 7d. The sedimentary formations instead, when alone, produce smaller amplitude maxima at a frequency of 0.5–0.6 Hz distributed along the profile, and when combined with the El Cobre formation they tend to shift the maximum to lower frequencies and closer to the source.

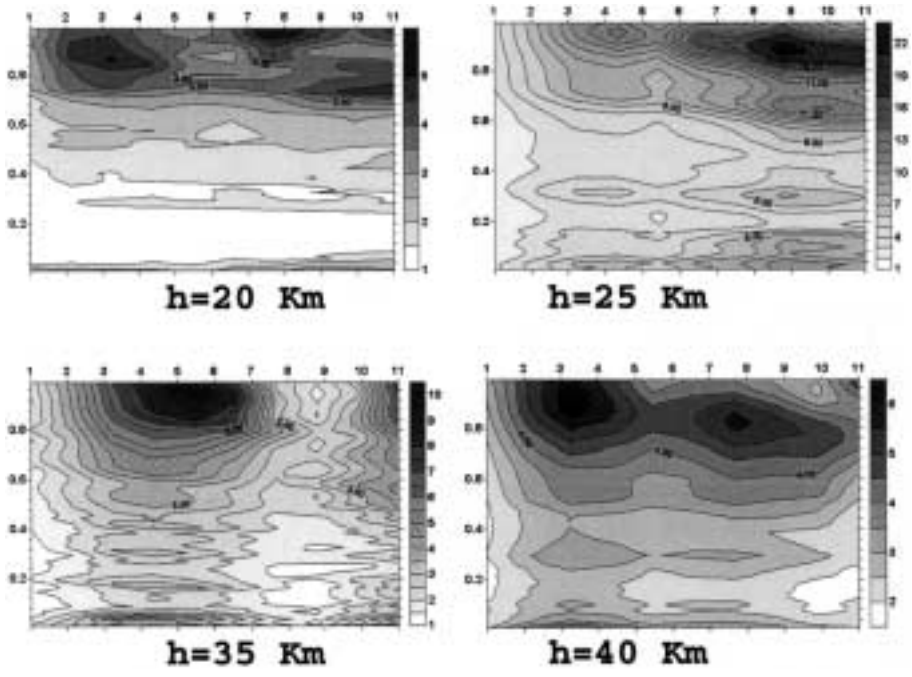

Figure 8
Test on depth of focus influence over signals. Response spectra ratio for radial *P-SV* waves along profile B.

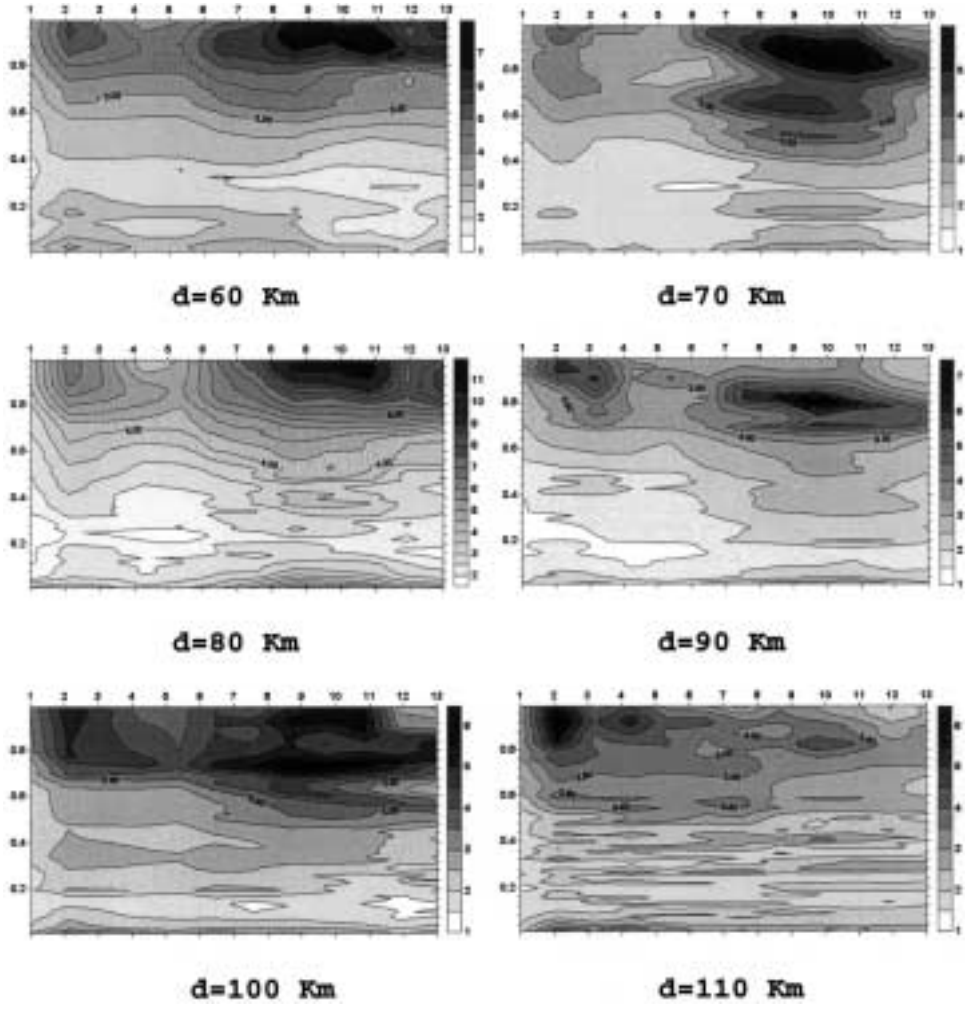

Figure 9
Test on source distance influence over signals. Response spectra ratio for radial *P-SV* waves along profile A.

We can therefore conclude that the large absolute maximum is due to waves critically reflected at the Moho and then polarised by the local strata, mainly those corresponding to La Cruz and El Cobre formations. Within our geometry such phenomena become relevant for distances stretching 60 to 120 km, and for focal depths ranging some 20 to 30 km. A similar effect is observed at distances as large as 150 km, however the small amplitudes of the waves involved (almost four times smaller than those at 80 km) make this effect irrelevant for our purposes.

The critical reflection effect has been detected in real data by other authors. BURGER *et al.* (1987) found that in North America the pseudo-velocity calculated at

1 Hz and 5% of damping does not obey a simple distance-decay law, although in the distance range of 60–150 km remains approximately constant, if not increasing, with increasing distance. In the course of time, KAWASE and AKI (1990) explained an unexpected major damage at the slope of Puente Hills (much greater than at the top of the hills) during the Whittier Narrows, California, earthquake of October 1, 1987 ($M_L = 5.9$), by sharp amplification of plane *SV*-waves incidence at the critical angle.

7.2. Comparison with Previous Seismic Microzoning Results

Our results may be compared with previous seismic microzoning of Santiago de Cuba, made by GONZÁLEZ *et al.* (1989), GONZÁLEZ (1991) and ZAPATA (1996). The first two investigations, mainly based on an analysis of the engineering-geological conditions of the city and on the measurements of microseisms (vertical velocity) in the frequency bands centered at 0.31, 0.62, 1.28, 2.5, 5, 10 and 27 Hz, supply two different maps, one with intensity variation estimates based on engineering-geological soil conditions and the other showing the predominant frequency of the measured microseisms. ZAPATA (1996), with the aid of a GIS system, reanalysed all the information contained in the two papers by GONZÁLEZ *et al.* (1989) and GONZÁLEZ (1991) and added the results of microseism measurements (3-component displacement) in the frequency range (0.6–6 Hz), as well as other geomorphological and geological data. ZAPATA (1996) produced a new microzoning map which divides the study area into five categories, and he supplied a somewhat fuzzy correlation with the expected variations of the macroseismic intensity. In Figures 10a and 10b we report the map of intensity variations of GONZÁLEZ *et al.* (1989) (map G1 in the following) and the microzoning map of ZAPATA (1996) (map Z in the following), together with the trace of profiles A and B and the position of the sites where we computed the synthetic seismograms. By simple inspection of the maps it is clear that their characteristics along the profiles are different. In the case of map G1 both profiles begin from a high level of seismic hazard and gradually pass to a low one. This is not the case for map Z. In this map profile A crosses a zone with a complicated pattern, and it is not possible for some sites to determine the exact category, while profile B crosses a zone with almost constant, low-level, seismic hazard.

The peak values of the ground motion indicate an acceptable agreement in the general trend along both profiles in the case of map G1, while for map Z the agreement is, in general, considerably worse, even if the differences are within one degree of intensity. The gradients in seismic intensity in G1 and Z maps are larger than those derived from synthetic seismograms, probably because of the difference in the cut-off frequency of the different data sets: 1 Hz for synthetic signal and 27 Hz for G1 and Z maps. The analysis of this problem will be the subject of a future investigation. However, the main difference between G1 and Z maps on one side, and our results on the other, is the effects due to critical reflections. These effects are entirely neglected in G1 and Z maps, because the procedure followed in their

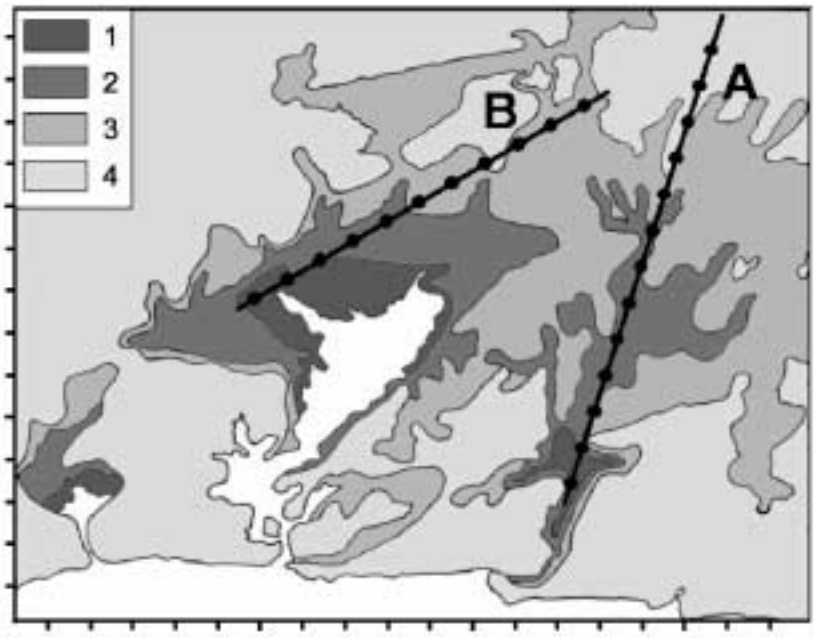

Figure 10a
Seismic microzoning maps of Santiago de Cuba: a) Modified from GONZÁLEZ *et al.* (1989), as a function of intensity increments [1 – $\Delta I \geq 1$, 2 – $\Delta I = 1$, 3 – $\Delta I = 0$, 4 – $\Delta I = -1$]. b) Modified from ZAPATA (1996) [1 – very favourable, 2 – favourable, 3 – middle, 4 – unfavourable, 5 – very unfavourable]. With respect to intensity, the classification of ZAPATA (1996) is {(1, 2) – $\Delta I = (-0.5, -1)$, 3 – $\Delta I = (0, 1)$, (4, 5)–ΔI = (1, 2 or more)}. Profiles and sites, ordered from SW to NW, of our computations are indicated with solid lines and full circles, respectively. The divisions on borders correspond to 1 km distance, and the left-lower corners have coordinates 19.956°N and 75.933°W in the case (a) and coordinates 19.954°N and 75.878°W in the case (b).

compilation does not take into account the propagation trajectory of the waves from the possible sources to the city.

Both G1 and Z maps have been compiled generalising a very limited data set, thus it is very unlikely that the discrepancies between these maps and our computations could be attributed to unaccounted 3-D effects, for the computation of which the quantity and quality of available structural data are totally inadequate. On the other hand, estimates based on 2-D models are able to explain, in general, the amplifications derived from real records, failing only in reproducing observations in restricted zones of the model and in limited frequency bands. This could be connected to unresolved structural features in the 2-D models at the related wavelength scales or to local 3-D effects (e.g., MARRARA and SUHADOLC, 2000). Modelling of 3-D structures, in practice, can only be done in theoretical applications or at very long periods, since detailed (few hundreds of meters resolution) 3-D structural models are not available at present, and will not be in the future, with scarce exceptions.

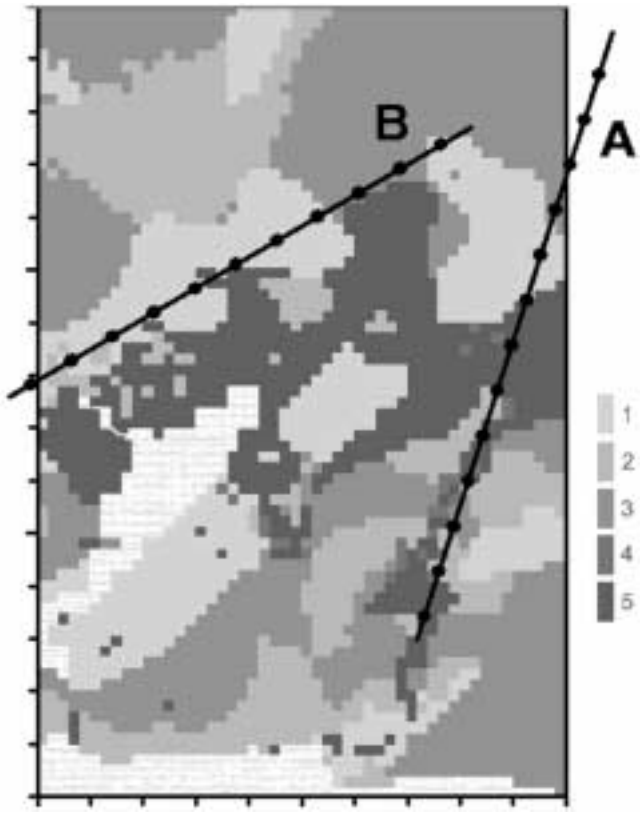

Figure 10b

8. Conclusions

Considering as scenario earthquakes two $M_s = 7$ events, representative of a seismogenic zone immediately south of the city, the Oriente fault zone, we study, along two profiles crossing Santiago de Cuba city, the influence of the regional structure and of the local soil conditions on ground motion.

In the cases of radial *P-SV* waves generated by a source located in a depth range of 20 to 30 km, at an epicentral distance ranging from 60 to 120 km, we observe, in the frequency interval 0.8–1 Hz, a strong amplification effect along the profile located North of Santiago de Cuba Bay. For the second profile the same phenomenon is observed in the range of distances from 70 to 90 km. This effect is due to waves critically reflected at the Moho and then polarised by the local strata, mainly those corresponding to La Cruz and El Cobre formations.

Where comparable, our results follow the general trend of the previous investigations considered, and the differences between our estimates of intensity

variation and those reported in maps G1 and Z are within one degree of intensity. The effect of the critical reflection evidenced by our analysis cannot be accounted for by the procedure followed by GONZÁLEZ *et al.* (1989) and ZAPATA (1996).

Acknowledgements

This work was partially supported by ICTP grants (TRIL Programme and the Associateship Programme) and from IUGS-UNESCO-IGCP Project 414: "Realistic Modelling of Seismic Input for Megacities and Large Urban Areas."

REFERENCES

AKI, K., *Strong motion seismology*. In *Strong Ground Motion Seismology, NATO ASI Series, Series C: Mathematical and Physical Sciences,* vol. 204 (eds. Erdik, M. Ö. and Toksöz, M. N.) (D. Reidel Publishing Company, Dordrecht, 1987), pp. 3–41.

ALVAREZ, L., VACCARI, F., and PANZA, G. F. (1999), *Deterministic Seismic Zoning of Eastern Cuba*, Pure appl. geophys. *156*, 469–486.

BURGER, R. W., SOMERVILLE, P. G., BARKER, J. S., HERRMANN, R. B., and HELMBERGER, D. V. (1987), *The Effect of Crustal Structure on Strong Ground Motion Attenuation Relations in Eastern North America*, Bull. Seismol. Soc. Am. *77*, 420–439.

FÄH, D. (1992), *A Hybrid Technique for the Estimation of Strong Ground Motion in Sedimentary Basins*, Ph.D. Thesis, Nr. 9767, Swiss Fed. Inst. Technology, Zürich, 161 pp.

FÄH, D., IODICE, C., SUHADOLC, P., and PANZA, G. F. (1993), *A New Method for the Realistic Estimation of Seismic Ground Motion in Megacities, the Case of Rome*, Earthquake Spectra *9*, 643–668.

FÄH, D., and SUHADOLC, P. (1994), *Application of Numerical Wave Propagation Techniques to Study Local Site Effects: The Case of Benevento (Italy)*, Pure appl. geophys. *143*, 513–536.

FIELD, E. H. (1996), *Spectral Amplification in a Sediment-filled Valley Exhibiting Clear Basin-edge-induced Waves*, Bull. Seismol. Soc. of Am. *86*, 991–1005.

FLORSCH, N., FÄH, D., SUHADOLC, P., and PANZA, G. F. (1991), *Complete Synthetic Seismograms for High-frequency Multimode SH-waves*, Pure appl. geophys. *136*, 529–560.

GONZÁLEZ, B. E. (1991), *Estimación del efecto sísmico en la ciudad de Santiago de Cuba*, Tesis en opción al grado de Candidato a Doctor en Ciencias Físicas, Instituto de Geofísica y Astronomía, La Habana.

GONZÁLEZ, B. E., MIRZOEV, K. M., CHUY, T., GOLUBIATNIKOV, V. L., LYSKOV, L. M., ZAPATA, J. A., and ALVAREZ, H. (1989), *Microzonación sísmica de la ciudad de Santiago de Cuba*, Comunicaciones Científicas sobre Geofísica y Astronomía, No. 15, 25 pp., Instituto de Geofísica y Astronomía, Academia de Ciencias de Cuba.

GONZÁLEZ, B. E. (1998), *El método de los microsismos en la solución de tareas de la sismología ingenieril*, Memorias del III Congreso cubano de Geología y Minería (GEOMIN98), vol. I, pp. 284–286, Editorial Palcograf, ISSN 939-7117-01-0.

GUSEV, A. A. (1983), *Descriptive Statistical Model of Earthquake Source Radiation and its Application to an Estimation of Short-period Strong Motion*, Geophys. J. Roy. Astron. Soc. *74*, 787–800.

HEREDIA, N., SEISDEDOS, G., and Oliva, R. (1982), *Regionalización ingeniero-geológica de la cuenca de Santiago de Cuba a escala 1: 25.000*. Internal Report, ISPJAM-MES, Santiago de Cuba.

ISHIHARA, K., Chairman (1993), *The Thechnical Committee for Earthquake Geothechnical Engineering (TC-4) of the International Society for Soil Mechanics and Foundation Engineering, Manual for Zonation on Seismic Geotechnical Hazards,* The Japanese Society of Soil Mechanics and Foundation Engineering, 145 pp.

KAWASE, H., and AKI, K. (1990), *Topography effect at the Critical SV-wave Incidence: Possible Explanation of Damage Pattern by the Whittier Narrows, California, Earthquake of 1 October 1987*, Bull. Seism. Soc. Am., *80*, 1–22.

MARRARA, F., and SUHADOLC, P. (2000), *2-D Modeling of Site Effects along the "EURO-SEISTET" Array (Volvi Graben, Grece)*, Pure appl. geophys. submitted.

MINBAS (1989), *Investigaciones complejas para la ubicación de una central electronuclear en la provincia Holguín. Tomo 1: Trabajos Sismológicos. Libro 9, parte 2: Informe sobre los materiales del procesamiento de la red de estaciones sismológicas*, Internal Report, Ministry of Basic Industry, Cuba, 360 pp.

NORMA CUBANA (1999), *Propuesta de nueva norma cubana sismorresistente*, 110 pp. (draft).

ORIHUELA, N., and CUEVAS, J. L. (1993), *Modelaje sismogravimétrico de perfiles regionales del Caribe central*, Revista Ingeniería, Universidad Central de Venezuela *8*, 55–73.

PANZA, G. F. (1985), *Synthetic Seismograms: The Rayleigh Waves Modal Summation*, J. Geophys. Res. *58*, 125–145.

PANZA, G. F., CAZZARO, R., and VACCARI, F. (1997), *Correlation between Macroseismic Intensities and Seismic Ground Motion Parameters*, Annali di Geofisica *XL*, 1371–1382.

PANZA, G. F., VACCARI, F., and ROMANELLI, F. (1999), *The IUGS-UNESCO IGCP Project 414: Realistic Modeling of Seismic Input for Megacities and Large Urban Areas*, Episodes *22*, 26–32.

PANZA, G. F., ROMANELLI, F., and VACCARI, F. (2000), *Seismic Waves Propagation in Laterally Heterogeneous Elastic Media: Theory and Applications to the Seismic Zonation*, Advances in Geophysics, *43*, 1–95.

PANZA, G. F., VACCARI, F., COSTA, G., SUHADOLC, P., and FÄH, D. (1996), *Seismic Input Modelling for Zoning and Microzoning,* Earthquake Spectra *12*, pp. 529–566.

PAVLOV, O. Y., red. (1984), *Seismic Microzoning* (in Russian), Moscow, Nauka.

RIEPL, J., BARD, P.-Y., HATZFELD, D., PAPAIOANNOU, C., and NECHTSHEIN, S. (1998), *Detailed Evaluation of Site-response Estimation Methods across and along the Sedimentary Valley of Volvi (EURO-SEISTEST)*, Bull. Seismol. Soc. Am. *88*, 488–502.

ROMANELLI, F., and VACCARI, F. (1999), *Site Response Estimation and Ground Motion Spectral Scenario in the Catania Area*, J. Seismol. *3*, 311–326.

RUBIO, M. (1985), *The Assessment of Seismic Hazard for the Republic of Cuba*, Ph.D. Thesis, Institute of Geophysics, Science Academy of Czechoslovakia, Prague.

SEO, K., GONZÁLEZ, B. E., ARANGO, E. *et al.* (1998), *Past, present and perspective research on seismic microzoning in the cities of Santiago de Cuba and Havana*, Proceedings of the *Workshop to Exchange Research Information in the International Scientific Research Project* "Joints studies on seismic microzonation in earthquake countries", Tokyo Institute of Technology, Japan, 17 pp.

TRIFUNAC, M. D. (1977), *Methods for Prediction of Strong Earthquake Ground Motion*, Final Technical Report, October 1, 1976-September 30, 1977, prepared for the U.S. Nuclear Regulatory Commision, NUREG-0406, vol. 1.

ZAPATA, J. A. (1996), *Utilización de variantes metodológicas de microzonificación sísmica en la ciudad de Santiago de Cuba*, Tesis en opción al grado de Doctor en Ciencias Geofísicas, Centro Nacional de Investigaciones Sismológicas, Santiago de Cuba.

(Received March 16, 2000, accepted December 8, 2000)